

A MASTER CURVE-MECHANISM BASED APPROACH TO MODELING THE EFFECTS OF CONSTRAINT, LOADING RATE AND IRRADIATION ON THE TOUGHNESS-TEMPERATURE BEHAVIOR OF A V-4Cr-4Ti ALLOY

G. R. Odette, E. Donahue, G. E. Lucas, and J. W. Sheckherd (University of California, Santa Barbara)

OBJECTIVE

The objective of this work is to develop an understanding of fracture in the vanadium alloy system in support of quantitative methods for predicting failure of flawed fusion structures.

SUMMARY

The influence of loading rate and constraint on the effective fracture toughness as a function of temperature [$K_e(T)$] of the fusion program heat of V-4Cr-4Ti was measured using subsized, three point bend specimens. The constitutive behavior was characterized as a function of temperature and strain rate using small tensile specimens. Data in the literature on this alloy was also analysed to determine the effect of irradiation on $K_e(T)$ and the energy temperature (E-T) curves measured in subsized Charpy V-notch tests. It was found that V-4Cr-4Ti undergoes "normal" stress-controlled cleavage fracture below a temperature marking a sharp ductile-to-brittle transition. The transition temperature is increased by higher loading rates, irradiation hardening and triaxial constraint. Shifts in a reference transition temperature due to higher loading rates and irradiation can be reasonably predicted by a simple equivalent yield stress model. These results also suggest that size and geometry effects, which mediate constraint, can be modeled by combining local critical stressed area σ^*/A^* fracture criteria with finite element method simulations of crack tip stress fields. The fundamental understanding reflected in these models will be needed to develop $K_e(T)$ curves for a range of loading rates, irradiation conditions, structural size scales and geometries relying (in large part) on small specimen tests. Indeed, it may be possible to develop a master $K_e(T)$ curve-shift method to account for these variables. Such reliable and flexible failure assessment methods are critical to the design and safe operation of defect tolerant vanadium structures.

INTRODUCTION

Vanadium alloys are attractive candidates for structural applications in fusion reactors because of their low neutron activation, favorable thermal properties and potential for radiation stability. However, a potential problem that these alloys share with other body centered cubic (bcc) metals is a so-called ductile-to-brittle transition below a temperature (T_t) which may be significantly elevated as a consequence of irradiation. Preliminary studies using nonstandard tests -- including one-third-size, Charpy V-notch and disc bend specimens -- have suggested that alloy compositions in the range V-4Cr-4Ti are highly resistant to embrittlement, with T_t in the vicinity of or below -196°C (liquid nitrogen temperatures) even following high fluence irradiations and exposure to hydrogen¹⁻⁵.

However, T_t depends on the details of the test procedure⁶, and it cannot be used to quantify structural stress and strain limits; hence, it is neither a fundamental material property nor a useful engineering parameter. Indeed, while $K_e(T)$ is a useful quantitative measure of fracture resistance, it also depends on variables such as size scales and flaw geometry (mediating the stress intensity factor, crack tip energy release rate and constraint), loading(strain) rate, irradiation and other sources of embrittlement (e.g., hydrogen). As discussed in detail elsewhere⁷, it may be possible to develop a method to predict the stress and strain limits of flawed fusion structures using a master $K_e(T)$ curve adjusted on an absolute temperature scale using measured shifts (ΔT) to account for variables such as constraint (ΔT_c), irradiation (ΔT_i) and strain rate ($\Delta T_\dot{\epsilon}$): that is,

$$K_e(T) = K_{mc}(T - [T_0 + \Delta T_c + \Delta T_i + \Delta T_{\dot{\epsilon}} + \Delta T_m]) \quad (1)$$

where T_0 is a reference temperature at a valid reference K_{Jc} level (e.g., 60 MPa \sqrt{m}) and ΔT_m is a specified safety margin.

In addition to developing the master curve-shift method for vanadium structures, the broader objective of this research is to integrate measurements of $K_e(T)$ with observations of fracture processes and modeling to: 1) determine the basic fracture mechanisms and obtain a fully quantitative micromechanically-based local fracture model; 2) develop methods to use small specimens to measure the intrinsic fracture resistance of these alloys; 3) determine methods to use the intrinsic properties of these alloys (note, $K_e(T)$ is not an intrinsic property) to predict load-displacement limits of flawed fusion structures; and 4) develop microstructure-property-property models of the effects of metallurgical variables and irradiation on fracture toughness.

EXPERIMENT

The study was carried out on the program heat of V-4Cr-4Ti (#832665) procured from Teledyne Wah Chang by Argonne National Laboratory⁸. Three-point bend tests were carried out on 1/3-sized Charpy V-notch specimens (3.33 x 3.33 x 25.4 mm) provided by Oak Ridge National Laboratory. The subsized Charpy specimen blanks were electro-discharge machined from 3.8 mm thick plate in the 40% warm-rolled (400°C) as-received condition with a T-L orientation (crack propagation parallel to the rolling direction). The machined specimens were annealed for 2h at 1000°C in a vacuum of better than 10⁻⁴ Pa to produce a recrystallized microstructure and remove residual hydrogen. This series of heat treatments produces an average grain size of about 25 μ m and a Vickers microhardness of about 150 \pm 5^{9,10}.

Fatigue pre-cracking was carried out at a final $\Delta K \leq 15$ MPa \sqrt{m} to a nominal crack length (a) to specimen width (W) ratio of $a/W \approx 0.5$. Considerable care was taken to insure that the pre-cracked miniature Charpy specimens (PMC) were kept well below their yield load. Side grooves were machined into subset of the PMC specimens with a dry abrasive cutting wheel; the side grooves had root radii of about 0.25 mm and a depth of about 0.1W on each side. A third set of PMC specimens was fatigue pre-cracked on each side from shallow notches to a depth of about 0.1W. Side notched specimens (PNC) and side pre-cracked specimens (PPC) had increased lateral (plane strain) constraint following general yielding compared to the smooth sided (PMC) specimens. The specimens were tested in three point bending over a temperature range from -196 to 21°C at approximate loading rates of 8.8 x 10⁻⁶ m/s (static, S), 0.3 m/s (low dynamic, LD) and 3 m/s (intermediate dynamic, ID).

Due to the very small size of the specimens combined with the relatively low strength of the V-4Cr-4Ti alloy (e.g., a room temperature yield stress (σ_y) of about 350 MPa) the only true fracture events that were observed were cleavage pop-ins that occurred at low temperatures below a (varying) sharp transition. Roughly semicircular pop-in cleavage cracks were pinned and arrested at various distances towards the sides and back of the specimen. At only slightly higher temperatures, fracture was generally not observed. In this case, the specimen responded to the applied load by massive crack blunting and bending until it simply bottomed out in the test fixture. A limited amount of stable crack tearing was observed in at least one case at a K_e greater than about 300 MPa \sqrt{m} .

In a few cases (e.g., low-dynamic loading rates at very low temperature and the static test at -196°C) a standard K_e could be determined from $K_e = \sqrt{J_{Ic} E'}$, where E' is the plane strain elastic modulus and J_{Ic} is the critical effective energy release rate given by the area under the stress-displacement (time) curve up to the load drop at cleavage pop-in. However, determining J_{Ic} from load-displacement/time data was not generally possible. In these cases, K_e was evaluated from $K_e = \sqrt{\delta^* \sigma_y E'}$ where δ^* is the critical crack tip opening displacement at the point of initiation of crack extension^{11,12}. A confocal microscopy (CF)-

fracture reconstruction (FR) technique was used to measure δ^* . The FR algorithms use conjugate fracture surface topographs measured with CM to resolutions around 1 μm to tomographically determine the sequence of deformation and microfracture events in the process zone in front of the crack tip ultimately leading to macroscopic fracture (e.g., a macroscopic pop-in). The CM-FR method is described elsewhere^{11,12}. In cases where both could be compared, the two methods of estimating K_{e} were in good agreement. In addition to CM-FR, the fracture surfaces of all of the specimens were characterized by optical and scanning electron microscopy (SEM).

As-received, 1.07mm-thick sheets from the same heat of V-4Cr-4Ti were cold rolled (less than 5% per pass) to a thickness of 0.5mm with an intermediate heat treatment (at 0.86 mm) at 1000°C for 2h in vacuum. Miniature tensile specimens (25mm long) were punched from the 40% cold worked sheet with their axis perpendicular to the plate rolling direction. They were then given a final heat treatment at 1000°C for 2h in vacuum. The grain sizes and diamond pyramid hardness of the tensile specimens in this condition were roughly the same as the fracture specimens. A nearly complete matrix of tensile tests was conducted at temperatures from -196°C to 100°C in roughly 100°C intervals at estimated strain rates of about 4×10^{-4} , 2×10^{-2} and 2 s^{-1} . Load-cross head displacement data were analyzed to determine the engineering stress-strain $[\sigma(\epsilon)]$ curves. Previous measurements have shown that this expedient provides values of yield stress (σ_y) and ultimate tensile strength (σ_u) that are similar to those measured with methods using direct extensometry (of course, the apparent moduli and yield strains are greatly decreased and increased, respectively, by the load train compliance in the tests without direct extensometry). In most cases, a sharp well-defined σ_y was observed, and σ_y was defined at the Luders plateau if one was present. When a Luders plateau was not present, σ_y was defined at the 0.2% offset strain. The accuracy of σ_y was estimated to be about ± 15 MPa for the static tests and about ± 30 MPa at the intermediate and high strain rates.

EXPERIMENTAL RESULTS

Tensile Properties

Figure 1 shows representative $\sigma(\epsilon)$ curves obtained as a function of strain rate and test temperature. In general, the $\sigma(\epsilon)$ behavior is complex and variously includes yield drops, Luders plateaus, regions of strain hardening and necking; and the overall $\sigma(\epsilon)$ curve is influenced by factors such as the specimen geometry, adiabatic heating and stress state. Hence, the simpler property, σ_y , is primarily used in this study. Nonetheless, some general observations about $\sigma(\epsilon)$ are pertinent. First, both σ_y and σ_u increase with decreasing temperature and increasing strain rate (see below). The strain hardening rate overall is very low, with strain hardening exponents estimated to be less than 0.1. However, the macroscopic ductilities, including uniform (UE) and total elongation (TE), are typical of structural alloys and do not appear to vary significantly over much of the test parameter range. Both TE and UE, however, do decrease at the lowest temperatures and highest strain rates, where the latter drops essentially to zero. Closer examination shows that, with the exception of several data points, there is a trend towards decreased UE with increased σ_y . This trend, associated with a corresponding decrease in the strain hardening rate, is clearly seen in Figure 2 which shows that the ratio σ_y/σ_u increases with increasing σ_y . The data for the intermediate and high rates overlap and fall only slightly above the low rate, static data at high σ_y . If the σ_y/σ_u ratio is taken as a rough measure of the post yield constitutive behavior, these results suggest that conditions that produce the same σ_y also result in similar overall $\sigma(\epsilon)$ behavior. The validity of this hypothesis, including the effects of irradiation hardening, will be examined in future research.

However, in the current work emphasis is on deriving a $\sigma_y(\dot{\epsilon}, T)$ correlation. As shown in Figure 3, similar to the behavior of bcc steels¹³, the σ_y data can be collapsed onto a common strain rate ($\dot{\epsilon}$) compensated temperature (T') scale defined by

$$T'(K) = T(K)[1 + C \ln(\dot{\epsilon}_0/\dot{\epsilon})]. \quad (2)$$

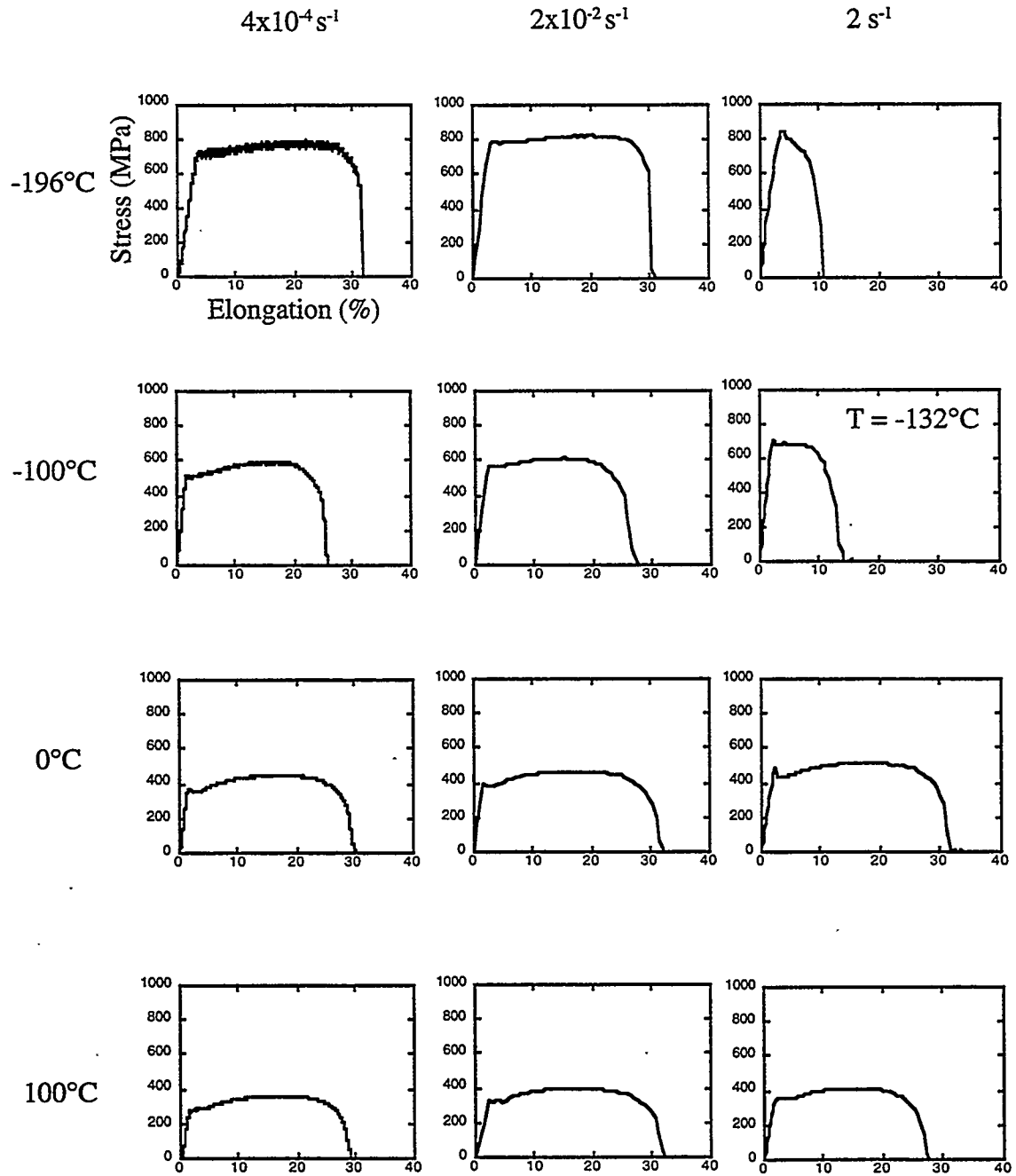


Figure 1. Examples of variation of stress-strain behavior with test temperature and strain rate.

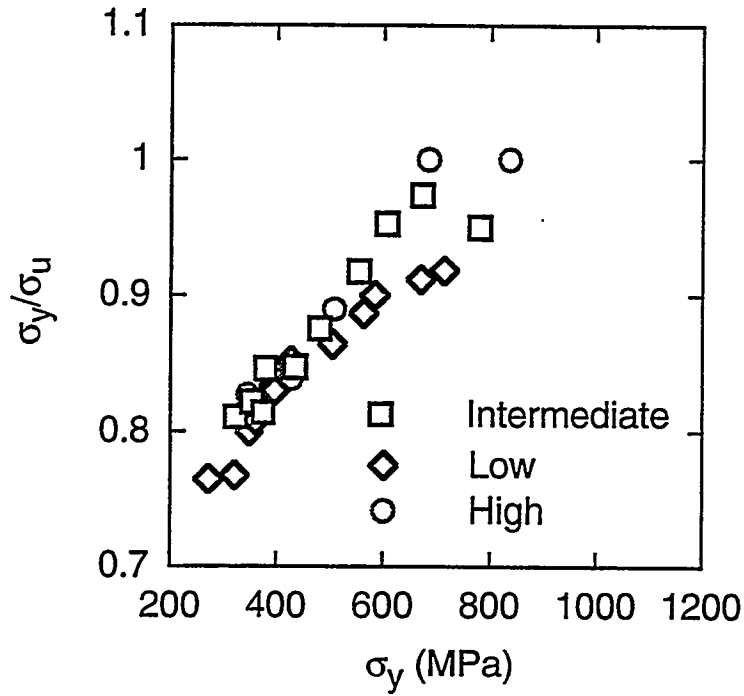


Figure 2 Variation of the ratio of yield stress to ultimate tensile strength with yield stress

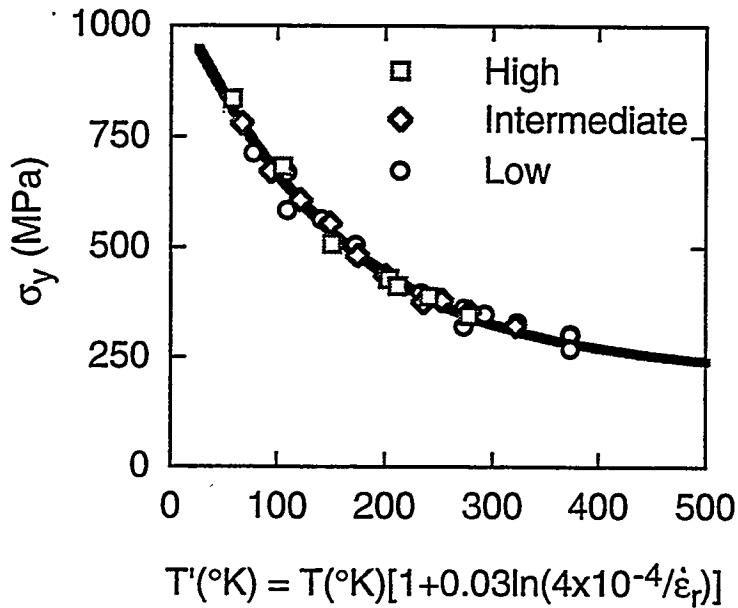


Figure 3 Variation of yield stress with strain-rate compensated temperature

When this is referenced at the lowest static rate, $\dot{\epsilon}_0 = 4 \times 10^{-4} \text{ s}^{-1}$ and $C = 0.03$. Thus, σ_y 's at high rates are equivalent to σ_y 's at static rates at a lower temperatures; e.g., $\sigma_y (2 \text{ s}^{-1}, 20^\circ\text{C}) \approx \sigma_y (4 \times 10^{-4} \text{ s}^{-1}, -27^\circ\text{C})$. The yield stress versus strain-rate-compensated temperature data in Figure 3 can be fit by an empirical polynomial as

$$\sigma_y(\text{MPa}) = 6.65 \times 10^{-9} T^4 - 1.53 \times 10^{-5} T^3 + 1.31 \times 10^{-2} T^2 - 5.22 T + 1070 \quad (3)$$

As discussed below, it will be critical to evaluate the effect of irradiation on the temperature and strain rate dependence, as well as the magnitude, of σ_y .

$K_e(T)$ Curves

Figure 4 summarizes the $K_e(T)$ data for the various specimen geometries (PMC, PNC, and PPC) and loading rates (S, LD, and ID). All fracture events that could be reliably measured occurred by cleavage with $50 \leq K_e \leq 200 \text{ MPa}\sqrt{\text{m}}$. The higher values of K_e , plotted at a "nominal" $300 \text{ MPa}\sqrt{\text{m}}$, denote the absence of cleavage and represent crude estimates of ductile fracture initiation toughness, which could not be measured in the small specimens used in this work. Figure 5 shows a SEM micrograph of the large cleavage pop-in for the S-PMC test at -196°C . The higher magnification views in Figure 6 show the predominance of cleavage in the pop-in region with some indications of a minor amount of intergranular fracture and subsurface cracking resulting in a plug-and-socket type of feature. A S-PMC test at -150°C produced only massive deformation and crack blunting as shown in Figure 7. However, as shown in Figure 8a the increased loading rate for the LD-PMC test resulted in a much higher brittle-to-ductile transition temperature (T_t) around -140°C . Increased lateral constraint provided by the side notching in the LD-PNC tests increased T_t to even a higher value of around -120°C , as shown in comparisons of Figures 8b and 8c. The additional lateral constraint from the sharp side pre-crack in the LD-PPC tests increased T_t slightly to about -110°C , as shown in comparisons of Figures 8d and 8e. Further increases in loading rate in the ID-PNC and ID-PPC specimen increased T_t to -110°C and -105°C , respectively. Again, the additional lateral constraint from the sharp side pre-crack in the ID-PPC tests increased T_t over that in the ID-PNC test, as seen by comparison of Figures 8f and 8g. The estimated values of T_t at of $60 \text{ MPa}\sqrt{\text{m}}$ are summarized in Table 1.

Table 1 - Variation of T_t with Constraint and Strain Rate

Loading Rate	Specimen (Constraint)	T_t ($^\circ\text{C}$)
S	PMC	-198 ± 5
LD	PMC	-140 ± 5
LD	PNC	-120 ± 5
LD	PPC	-110 ± 5
ID	PNC	-110 ± 5
ID	PPC	-105 ± 5

DISCUSSION OF LOADING RATE AND LATERAL CONSTRAINT EFFECTS

The variation of transition temperature with lateral constraint and strain rate and the very sharp transitions observed in these tests can be understood in terms of the (simplified) micromechanics of cleavage fracture⁷. For deep cracks in large specimens where plane strain, small scale yielding (SSY) conditions prevail, the

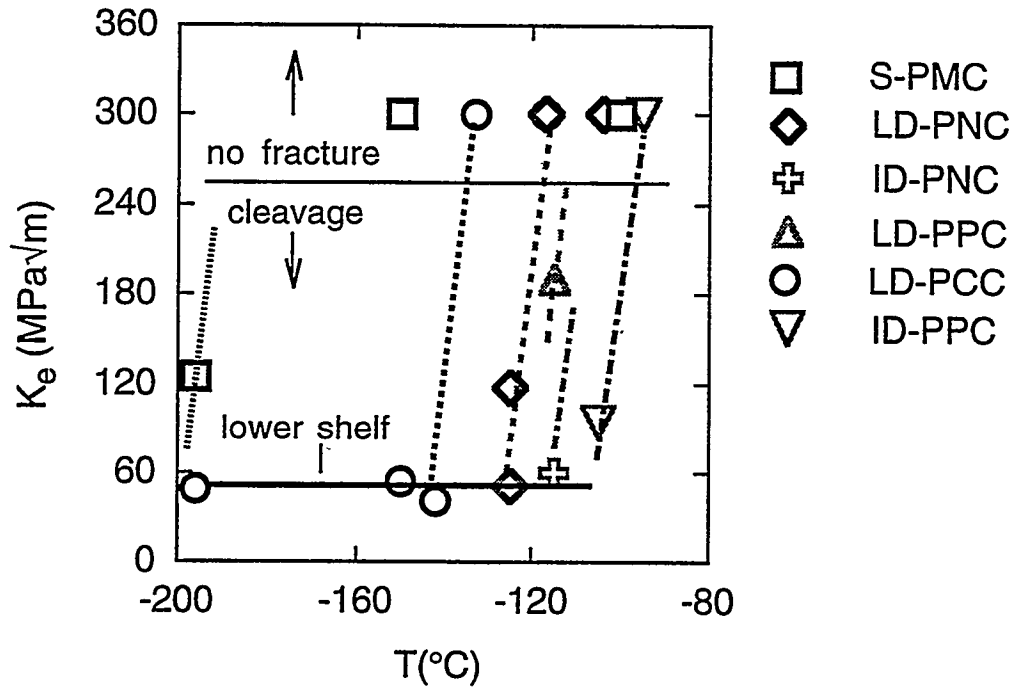


Figure 4 Variation of effective toughness with test temperature for various specimen types (PMC, PNC, and PPC) and loading rates (S, LD, and ID).

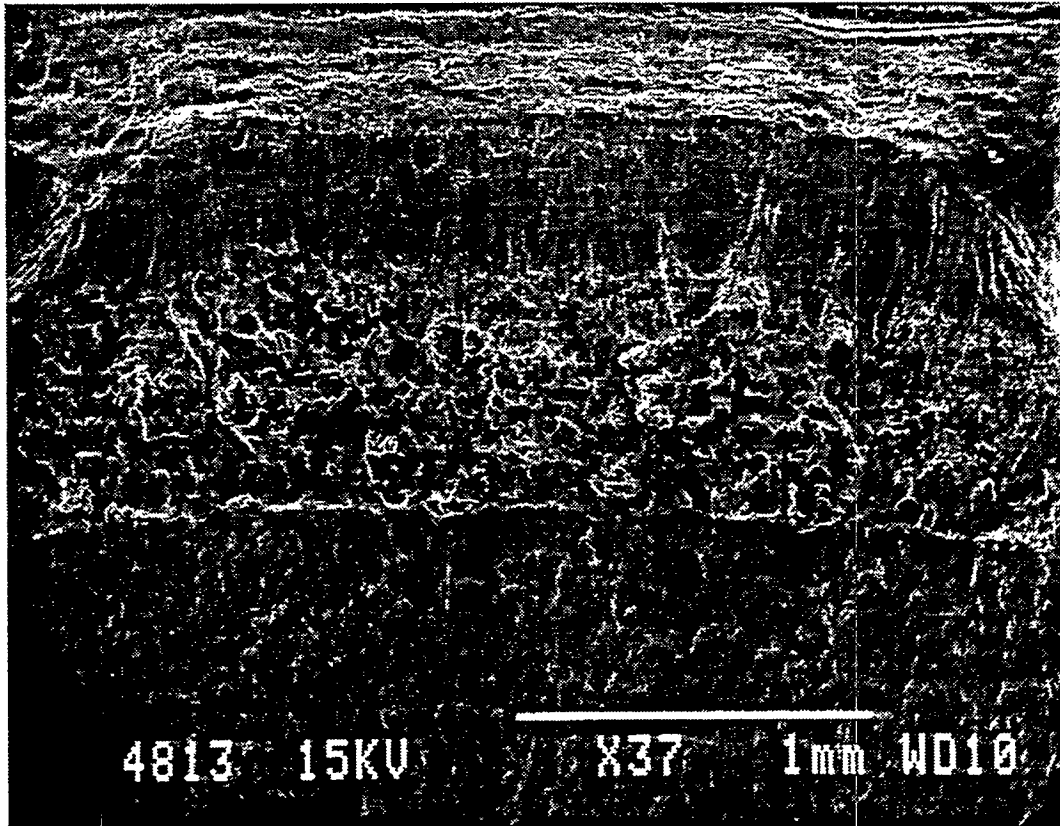


Figure 5. Low magnification SEM micrograph of the fracture surface of a PMC specimen tested statically at -196°C .

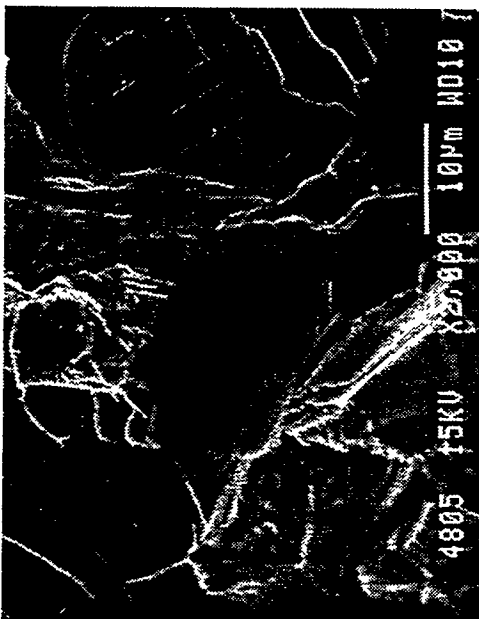
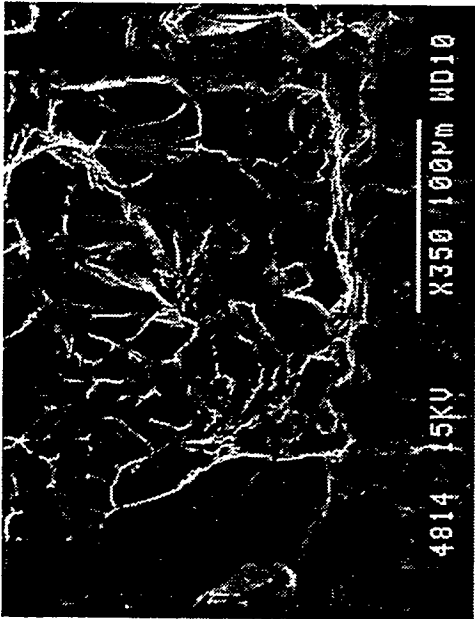
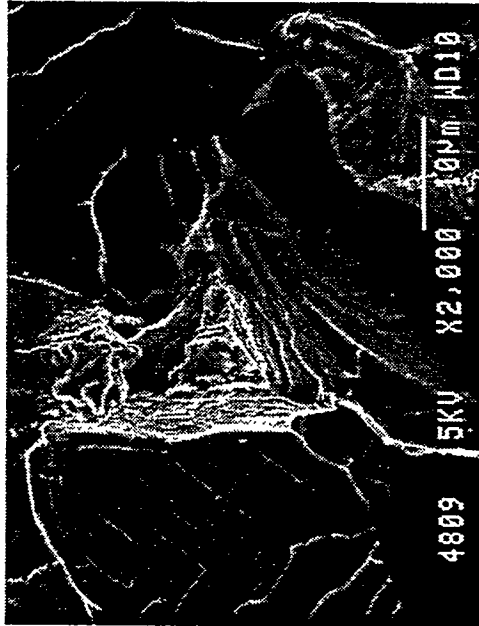


Figure 6. High magnification SEM micrographs of the cleavage fracture surface of a PMC specimen tested statically at -196°C.

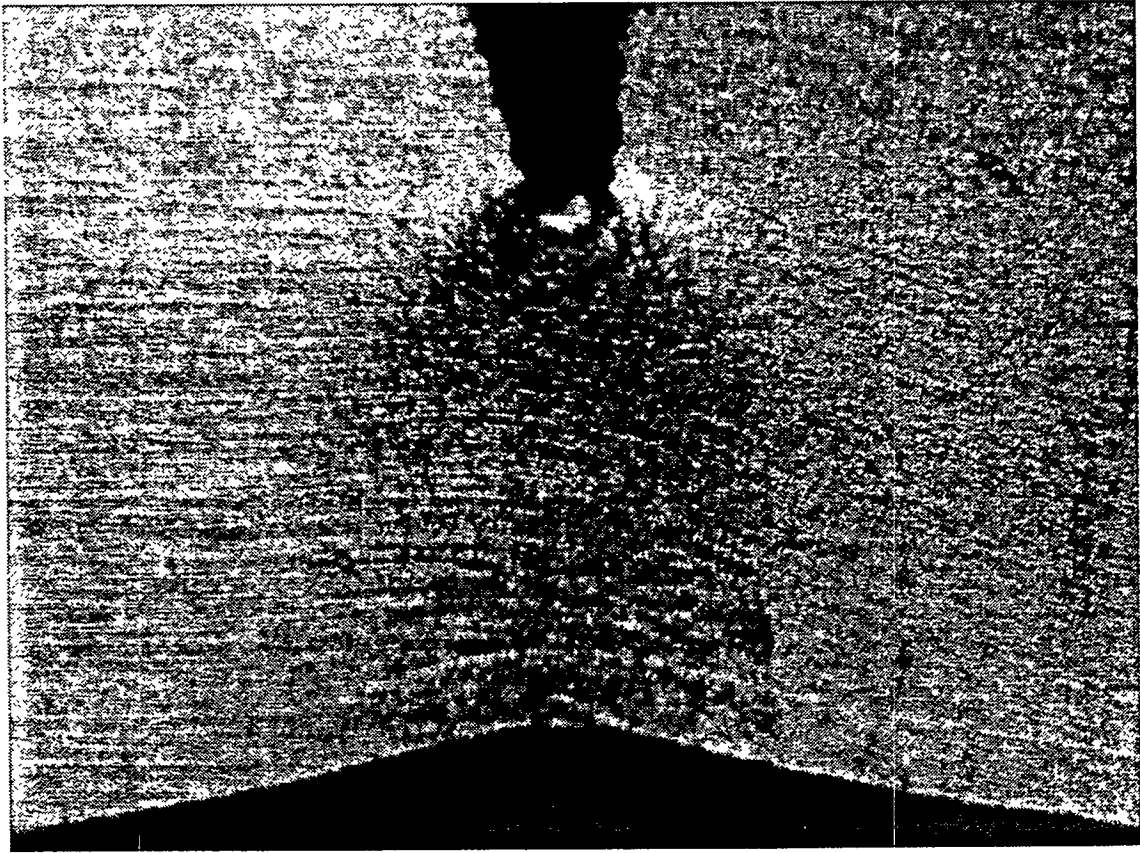


Figure 7. Side view of large deformation bending of PMC specimen tested statically at -150°C .

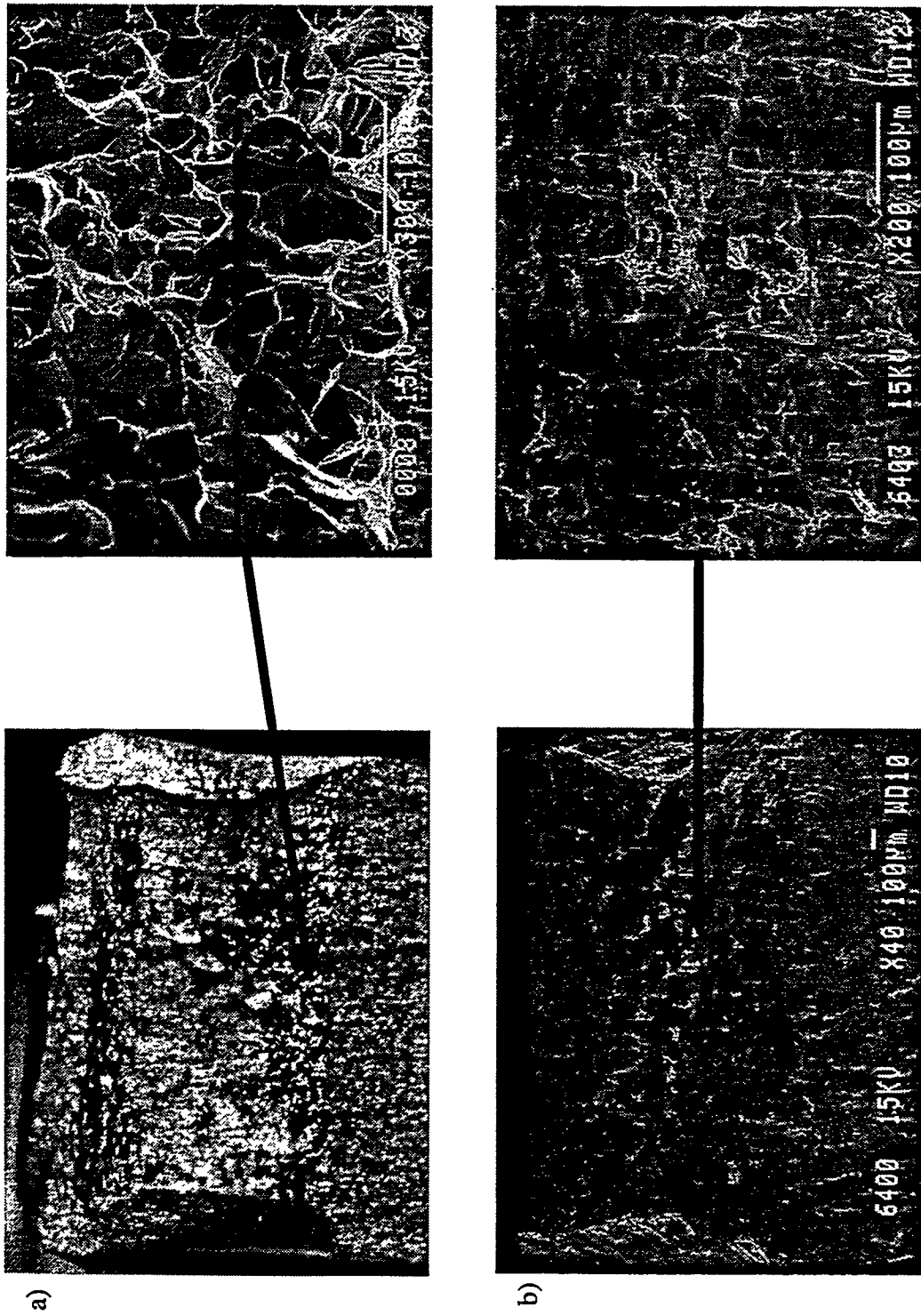


Figure 8. a) Low magnification optical and higher magnification SEM micrographs of LD-PMC specimen tested at -142°C; b) Low and high magnification SEM micrographs of LD-PMC specimen tested at -133°C.

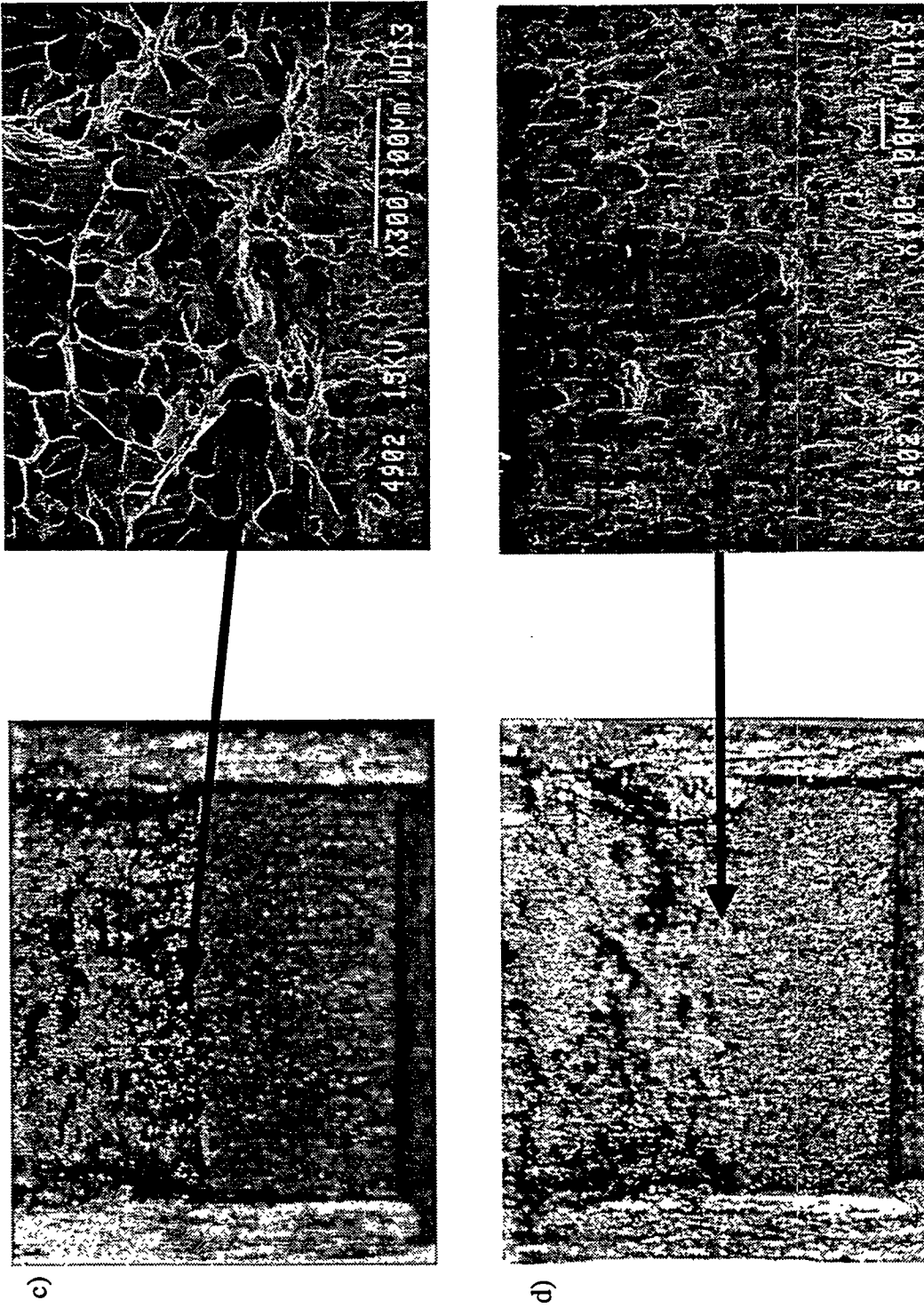


Figure 8. (cont.) Low magnification optical micrographs and higher magnification SEM micrographs of: c) LD-PNC specimen tested at -125°C; d) LD-PNC specimen tested at -117°C.

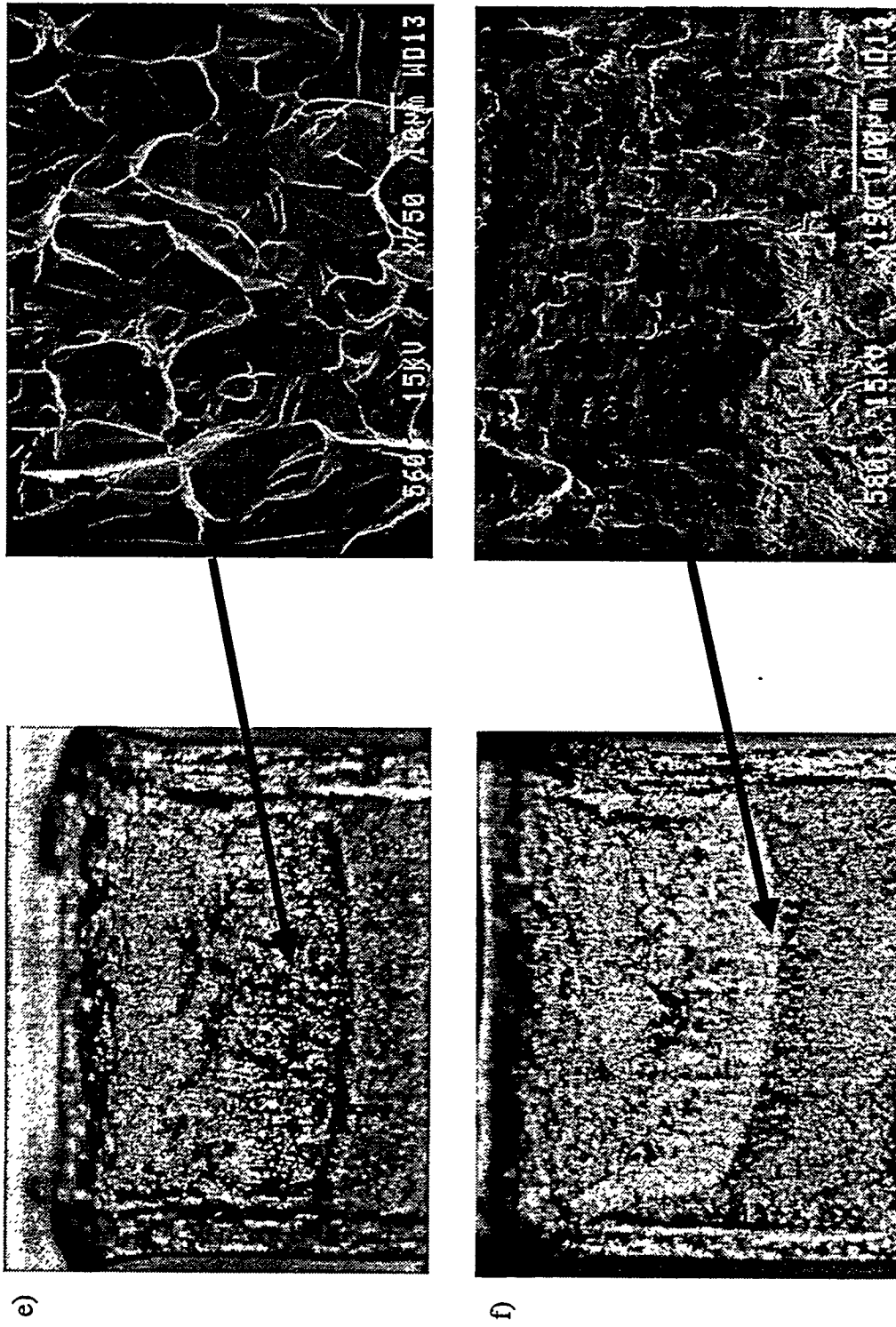


Figure 8. (cont.) Low magnification optical micrographs and higher magnification SEM micrographs of: e) LD-PPC specimen tested at -115°C; f) LD-PPC specimen tested at -105°C.

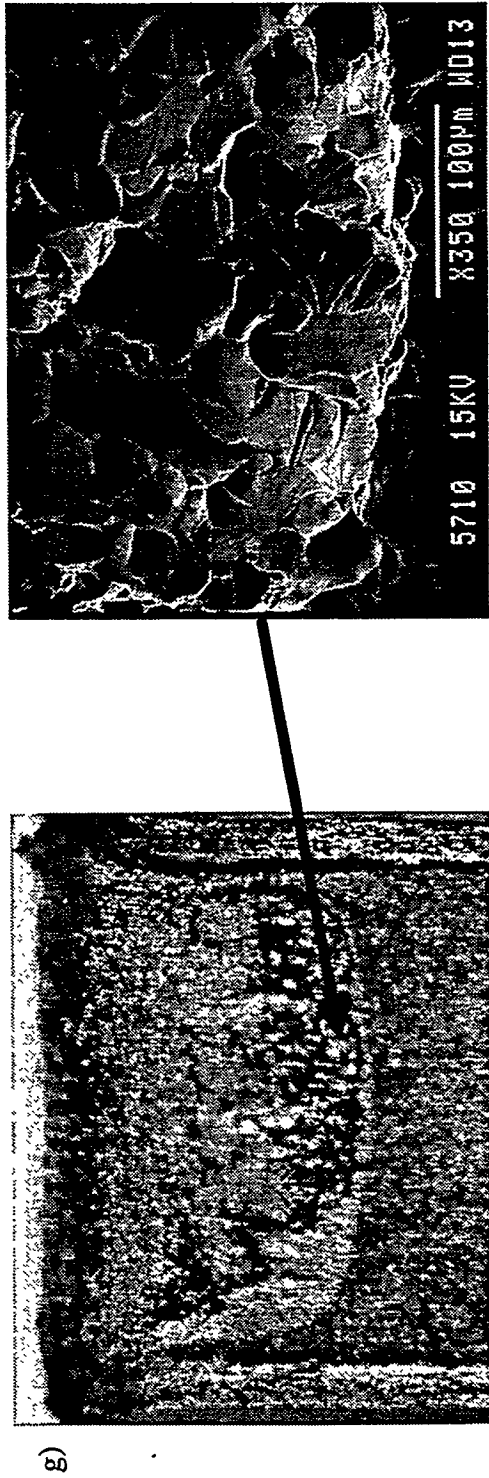


Figure 8. (cont.) g) Low magnification optical micrograph and higher magnification SEM micrograph of the ID-PNC specimen tested at -105°C.

peak tensile stress near the crack tip σ_t is a small multiple of the yield stress σ_y , with constraint factors $M_{SSY} = \sigma_t/\sigma_y$ of about 3 to 3.2 (note these constraint factors pertain to V alloys which have low strain hardening rates). In contrast, the maximum stress in specimens without a crack is approximately 1 to 1.2 σ_y . Cleavage and quasi-cleavage fracture are now believed to occur when the tensile stresses ahead of a crack tip exceed some critical value (σ^*) over a sufficiently large area (A^*)^{11,12,14}. Hence, σ^*/A^* are local measures of toughness that are intrinsic to the material and its microstructure. The onset of cleavage requires sufficiently low temperatures for $\sigma_t = M\sigma_y$ to exceed σ^* . Under SSY the area within a stress contour varies with the crack tip opening (δ) as δ^2 (or either K^4 or J^2 , where K is the linear elastic stress intensity factor and J is the elastic plastic crack tip energy release rate). Thus the crack must also blunt to a critical opening (δ^*) so that the $\sigma_t = M\sigma_y \geq \sigma^*$ occurs at $A \geq A^*$. Increasing strain rate (or irradiation hardening) increases σ_y , so the onset of cleavage occurs at higher temperatures.

For small pre-cracked specimens $M < M_{SSY}$. Thus a higher applied K is needed to reach the σ^*/A^* condition. Alternately, cleavage occurs at lower temperatures and/or higher strain rates where σ_y is higher. Thus the $K_{IC}(T)$ curves for subsized specimens are shifted down in temperature compared to the intrinsic $K_{IC}/J_{IC}(T)$ curves for deep crack, plane strain, SSY conditions. Loss of constraint under plane strain conditions occurs when plastic deformation reaches free surfaces in specimens with a small width (W) or short crack lengths (a), viz., when a or $W-a$ is less than about $100\delta^*$. However, constraint loss is also associated with lateral deformation in the direction of the specimen thickness (B) that occurs during crack blunting. Both sources of constraint loss reduce M and, hence, retard cleavage. Since the specimen W was fixed in this study, only the lateral plane strain constraint contribution could be increased by side notching or side pre-cracking. However, even these modest constraint enhancements resulted in T_t increases by 20 to 30°C.

The very sharp transition in the small pre-cracked specimens can also be understood based on these concepts, since: a) $d\sigma_y/dT$ is higher at lower temperature; b) $\delta(A^*/\sigma^*)$ increases with δ ; thus, an initial loss of constraint leads to even more loss of constraint before fracture; c) there is a loss of lateral plane strain conditions at larger deformation; and d) at high loading rates adiabatic heating after general yielding reduces the local yield stress and hence tensile stresses.

Similar concepts apply to impact tests on blunt Charpy V-notched specimens, with some modifications. First, the intrinsic constraint factor for notches (M_{CVN}) is smaller than for cracks: viz., $M_{CVN} \approx 2.2$. Further, beyond general yielding, the area within a stress contour scales roughly with the load (P)-deflection (Δ) energy and the root radius of the notch. For specimens with all dimensions (L) fully scaled, these vary as L^3 and L , respectively. Thus, the normalized energy (E_n , the P - Δ energy up to cleavage initiation divided by L^3)-temperature curve (E_n - T) required for cleavage (σ^*/A^*) is shifted down in temperature in small specimens even without large scale deformation. Further, cleavage is strongly retarded after general yielding by low strain hardening rates. Finally, the total energy measured in Charpy-type tests contains many contributions that have nothing to do with the fracture initiation process.

The inescapable conclusion from these results is that the low transition temperatures reported to date for V-4Cr-4Ti are largely a consequence of the relatively low yield stress and strain hardening of the alloy and the low constraint imposed by small, shallow blunt-notched Charpy specimens. Note that since the same material configured and tested in different ways showed a enormous range of T_t , the observation of brittle fracture in vanadium alloys cannot be attributed to impurity contamination. Indeed, it is estimated that for pre-cracked specimens sufficiently large to maintain plane strain SSY at cleavage fracture, the T_t for dynamic loading would be about -50°C or more. This is not much lower than T_t for the low activation, tempered martensitic steels that are also being considered for fusion structures.

More generally, these results demonstrate that great caution must be used in interpreting small specimen test data. Specifically, such tests may not only fail to provide "valid" data, but they may also not even "detect" important processes, such as cleavage, or even any type of fracture.

MODELING THE EFFECTS OF LOADING RATE AND IRRADIATION

In the case of bcc steel alloys, σ^* and A^* are known to be relatively insensitive to temperature, strain rate and the fine scale damage imposed by irradiation^{11,15}. If this is also the case for vanadium alloys, a simple way to model shifts in a reference transition temperature (ΔT_T) due to loading rate and irradiation hardening is to define transition temperatures at an *equivalent* reference σ_y . The appropriate reference condition is near the highest temperature of elastic cleavage fracture; this is at about $K_{Ic} = 60 \text{ MPa}\sqrt{\text{m}}$ in a pre-cracked specimen toughness test. Hence, ΔT_T can be modeled from a knowledge of the dependence of σ_y on temperature, strain rate and irradiation. In applying this model it is further assumed that: a) the overall $\sigma(\epsilon)$ for different temperatures, strain rates and levels of irradiation hardening ($\Delta\sigma_i$) are similar if the σ_y are the same; b) $\Delta\sigma_i$ is independent of temperature and strain rate; and c) Equations 2 and 3 provide an adequate description of $\sigma_y(\dot{\epsilon}, T)$ for the V-4Cr-4Ti alloy.

First, consider the effect of dynamic versus static loading rate on the PMC $T_t (= T_T)$ data given in Table 1. For the S-PMC test, $T_{RS} = 198 \pm 4^\circ\text{C}$; and for the ID-PMC test, $T_{RD} = -140 \pm 4^\circ\text{C}$; thus, $\Delta T_T \sim 58 \pm 6^\circ\text{C}$. For this case, the equivalent yield stress model (EYSM) gives $\Delta T_T = T_{RD} - T_{RS}$ where T_{RD} is related to T_{RS} by requiring

$$\sigma_y(\dot{\epsilon}_s, T_{RS}) = \sigma_y(\dot{\epsilon}_d, T_{RD}) \quad (4a)$$

Since the strain-rate-compensated temperatures are the same at the same yield stress, T_{RD} and T_{RS} are also related by

$$T(\sigma_{y,ref}) = T_{RS}[1 + C \ln(\dot{\epsilon}_0/\dot{\epsilon}_s)] = T_{RD}[1 + C \ln(\dot{\epsilon}_0/\dot{\epsilon}_d)] \quad (4b)$$

The effective strain rates for the PMC tests can be estimated by dividing the local strain at the peak stress location ahead of the crack (≈ 0.1) by the time to fracture ($\approx 60 \text{ s}$ for the S tests and 1 ms for the LD tests); this gives 1.7×10^{-3} and 96 s^{-1} , respectively. Using Equation 2, T' at T_{RS} (75K) for the S tests is 71.8°K and from Equation 3 the corresponding $\sigma_{y,ref}$ is 757 MPa . Solving Equation 4b, the value of T_{RD} at the same σ_y (and T') for the LD test is 115°K . Thus compared to the measured value of $58 \pm 6^\circ\text{C}$, the EYSM predicts a shift of about 40°C , a little smaller but of the right order.

The effects of irradiation on shift can also be predicted from $\Delta\sigma_i$ in a similar way: namely, $\Delta T_T = T_{Ti} - T_{Tu}$ when

$$\sigma_{yi}(T_{Ti}) = \sigma_{yu}(T_{Tu}) + \Delta\sigma_i \quad (5)$$

where the evaluation is at the pertinent strain rate.

Alexander and Snead¹⁶ have recently reported values of $\Delta\sigma_i$ and ΔT_T for the same heat of V-4Cr-4Ti for blunt notched (MCVN) and pre-cracked miniaturized Charpy specimens (1/3 cross section and 1/2 length) irradiated in HFBR to 0.5 dpa at about 110 to 235°C . The T_T for these MCVN tests is nominally at about 0.5 J (10J times the MCVN/CVN volume ratio). However, for a variety of reasons it is very difficult to establish T_T experimentally. Thus it was simply estimated by extrapolating the MCVN E-T curve in the transition region to zero energy, giving an estimated T_{Tu} of -205°C . The predicted ΔT_T versus $\Delta\sigma_i$ curve from Equations 2, 3 and 5 for a nominal strain rate of 100 s^{-1} is shown as the solid line in Figure 9a along with the experimentally observed shifts for the blunt notched MCVN specimens. Figure 9b shows a similar

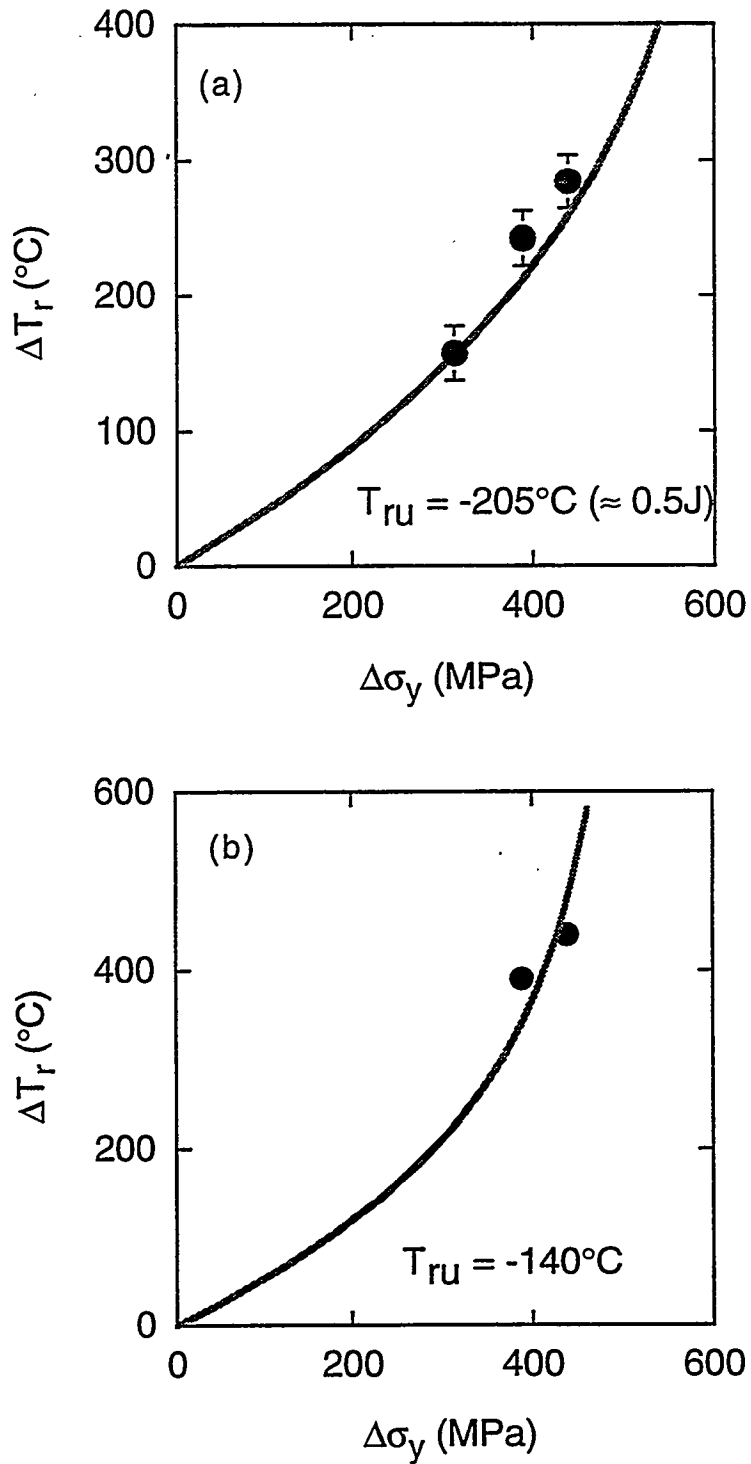


Figure 9 Shift versus hardening for a) blunt notched and b) pre-cracked MCVN specimens. The data points are taken from Alexander and Snead and the line is predicted from the equivalent yield stress model.

comparison for pre-cracked specimens. In both cases the predictions of the EYSM are in remarkably good agreement with the measurements. Notably, the ΔT_T for the pre-cracked MCVN tests are larger than the blunt-notched MCVN tests for the same $\Delta\sigma_I$; this is simply a consequence of the higher T_{TU} ($\approx -140^\circ\text{C}$) for the sharp crack versus the blunt notch specimens.

CONCLUSIONS

In summary, the data and analysis presented here demonstrate that the program heat of V-4Cr-4Ti undergoes a "normal" stress-controlled ductile-to-cleavage transition, typical of bcc alloys. The temperature marking this transition is strongly affected by constraint (experimentally demonstrated only for loss of plane strain constraint), loading rate and irradiation. Hence, the observations to date of the low transition temperature and embrittlement resistance of this alloy are primarily the result of the low yield stress of this alloy coupled with the relatively small constraint associated with small specimen sizes and blunt notches. This emphasizes that caution must be exercised in interpreting small specimen data. Not only may such small specimens lack the capacity to provide "valid" intrinsic properties, but they may even fail to detect real physical phenomena, such as cleavage.

The preliminary results also show that temperature shifts due to high loading rates and irradiation can be predicted using a very simple EYSM. The excellent quantitative agreement between the EYSM predictions and experiment also demonstrate the primary role of irradiation hardening in embrittlement of these alloys, and strongly contradicts alternate ad hoc explanations (e.g., impurity pickup). While not explicitly treated in this work, this research also suggests that the effect of specimen/structure size and geometry, that mediate constraint effects even under plane strain conditions, can be modeled by combining finite element method simulations of crack tip stress (and strain fields) with local fracture properties (e.g., σ^*/A^*). While additional research is needed, the present results are also very encouraging about the possibility of developing a powerful and practical master curve-shift method that is founded on physical understanding and complemented by basic measurements and models to reliably predict the stress and strain limits of flawed fusion structures.

ACKNOWLEDGMENTS

This work was supported in part by the Office of Fusion Energy, DOE, Grant No. DE-FG03-87ER-52143. The assistance of A. Rowcliffe and A. N. Gubbi of ORNL in specimen acquisition and preparation is gratefully acknowledged.

REFERENCES

1. B.A. Loomis, D. L. Smith, *J. Nucl. Mater.* 179-181 (1991) 783.
2. B. A. Loomis, D. L. Smith, F. A. Garner, *ibid.*, 771.
3. H. Chung, and D. L. Smith, *J. Nucl. Mater.*, 191-194 (1992) 942.
4. B. A. Loomis, L. J. Nowicki, J. Gazda, D. L. Smith, *Fusion Reactor Materials Semiannual Progress Report, DOE/ER-0313/15, March 31 (1993) 318.*
5. B. A. Loomis, H. M. Chung, L. J. Nowicki, D. L. Smith, *J. Nucl. Mater.*, 212-215 (1994) 799.
6. K. Edsinger, G. R. Odette, G. E. Lucas, J. W. Sheckherd, *Proceedings of the 7th Int'l Conference on Fusion Reactor Materials, J. Nucl. Mater.* (in press)

7. G. R. Odette, Proceedings of the IEA/JUPITER Symposium on Small Specimen Test Technologies for Fusion Materials, Sendai, Japan, March 1996.
8. H. M. Chung, H.-C. Tsai, D. L. Smith, R. Peterson, C. Curtis, C. Wojcik, and R. Kinney, Fusion Reactor Materials Semiannual Progress Report, DOE/ER-0313/17, March (1994).
9. M. L. Grossbeck, D. J. Alexander, J. J. Henry, W. S. Eatherly, L. T. Gibson, Fusion Reactor Materials Semiannual Progress Report, DOE/ER-0313/18, March (1995).
10. A. N. Gubbi, A. F. Rowcliffe, W. S. Eatherly, *ibid.*
11. K. Edsinger, G. R. Odette, G. E. Lucas, B. Wirth, ASTM-STP-1270, American Society for Testing and Materials, Philadelphia, PA (in press)
12. K. Edsinger, G. R. Odette, G. E. Lucas, Proceedings of the IEA International Symposium on Miniaturized Specimens for Testing Irradiated Materials, KFA Julich, September 22-23, 1994 (1995) 150-159.
13. J. M. Steichen and J. A. Williams, *J. Nucl. Mater.*, 57 (1975) 303.
14. G. R. Odette, *J. Nucl. Mater.*, 212-215 (1994) 45.
15. K. Edsinger, PhD Thesis, Department of Chemical Engineering, UCSB (1996).
16. D. J. Alexander and L. Snead, presented at the 18th International Symposium on Effects of Radiation on Materials, ASTM, Hyannis, Massachusetts, June, 1996.